Pressure Dependence of Negative Hydrogen Ion Production in a Cesium Seeded Tandem Volume Source

Osamu FUKUMASA and Eiji NIITANI

Department of Electrical and Electronic Engineering,
Faculty of Engineering, Yamaguchi University, Ube 755, Japan

(Received June 12, 1996; accepted for publication September 25, 1996)

Effects of cesium vapor injection on H^- production in a tandem volume source are studied numerically as a function of plasma parameters. Model calculation is performed by solving a set of particle balance equations for steady-state hydrogen discharge plasmas. Here, the results with a focus on gas pressure and electron temperature dependences of H^- volume production are presented and discussed. Considering H^- surface production caused by both H atoms and positive hydrogen ions, enhancement of H^- production and pressure dependence of H^- production observed experimentally are qualitatively well reproduced in the model. For enhancement of H^- production, however, so-called electron cooling is not very effective if plasma parameters are initially optimized with the use of a magnetic filter.

KEYWORDS: tandem negative ion source, source modeling, magnetic filter, volume production, vibrationally excited molecules, cesium vapor injection, surface production

1. Introduction

Sources of H^- and D^- ions are required for generation of efficient neutral beams with energies in excess of 150 keV. The magnetically filtered multicusp ion source has been shown to be a promising source of high quality, multi-ampere H^- ions. In pure hydrogen discharge plasmas, most of the H^- ions are produced by the two-step process which involves dissociative attachment of slow plasma electrons, e (with electron temperature, T_e ~ 1 eV) to highly vibrationally excited hydrogen molecules, $H_2(v)$. Recent experimental investigations have revealed that the addition of cesium (Cs) or barium to a hydrogen discharge can enhance the H^- output current by a several factor and cause a substantial reduction in the electron-to-H^- ratio in the extracted beam.[1,2] It has also been reported[3,4] that the optimum pressure, p_{opt}, giving the highest H^- current for a certain arc current (I_a) is almost independent of I_a and that the value of p_{opt} decreases to 0.8-1.0 Pa when Cs vapor is seeded into a plasma source. Although these effects have been observed by many researchers, the mechanism of Cs catalysis in H^- production remains to be clarified.

To date, we have studied source modeling[5,6] and Cs effects on enhancement of H^- yield.[7] The mechanisms underlying Cs injection enhancement of H^- production are reported to be as follows:[1,8] (1) Electron cooling, (2) Production of $H_2(v)$ due to reaction between Cs atoms and H_2^+, and (3) H^- surface production caused by H atoms and positive hydrogen ions. Based on some experimental results (for example, correlation between the H^- current and the work function of the plasma grid[9] and dependence of H^- current on barium washer voltage[10]), we assume that the dominant process of enhancement is surface production, where the surface has a low work function because of the Cs coverage. In this paper, to elucidate further the Cs effects, we will discuss enhancement of H^- yield as a function of some plasma parameters, i.e. electron

density n_e, hydrogen gas pressure p and T_e. Taking into account H^- surface production, the model calculation well reproduces the characteristic features on enhancement of H^- production observed experimentally.[3,4]

2. Simulation Model

To study H^- production in a tandem two-chamber system, we used the simulation model[5,6] shown in Fig. 1. Two chambers of volume $L_1 \times L \times L$ (the first) and $L_2 \times L \times L$ (the second) are in contact with each other in the region of the magnetic filter, where $L = L_1 + L_2 = 30$ cm. We assume that fast electrons, e_f are present only in the 1st chamber because the magnetic filter prevents e_f from entering the 2nd chamber. We consider four ion species (H^-, H^+, H_2^+ and H_3^+), two electron species (e and e_f) and three species of neutral particles [H, $H_2(v'')$ and H_2]. Particles other than e and e_f are assumed to move freely between the two chambers without being influenced by the filter. The number of particles passing through the filter is represented by flux nv, where n and v are the particle density and velocity, respectively.

In the present model, two kinds of reaction process at the wall surface are included. One is H^- surface production caused by Cs injection. The following four processes are considered:[7,11] H_n^+ + wall → nH^- (n = 1,2,3), and H + wall → H^-. The other is the effect of $H_2(v'')$ surface production due to wall recombination of H and neutralization of positive ions.[12,13] Wall effects considered here are summarized in Fig. 2.

In modeling, surface production rates of negative ions are estimated as follows. The term representing wall loss of H atoms is expressed as $-(\gamma_1 + P_{CsH})N_H / \tau_H$, where γ_1 is a wall recombination coefficient, P_{CsH} indicates the probability of H^- formation at the wall, N_H is H density, and τ_H is a confinement time of H. Then, the H^- production rate at the wall surface is expressed as $P_{CsH} N_H / \tau_H$. We also assume that recombination of H to H_2 at the

wall is written as $\gamma N_H (2\tau_H)^{-1}$. Therefore, production of $H_2(v'')$ is expresses as $P_{eq} \gamma N_H (2\tau_H)^{-1}$, where P_{eq} is the probability of finding $H_2(v'')$ in H_2 formed at the wall. In the same way, the rates of production of H^- and $H_2(v'')$ from positive ions at the wall are also estimated.

For each chamber, 19 rate equations for H, $H_2(v''=1\text{-}14)$, H^-, H^+, H_2^+ and H_3^+ are derived by taking into account the above-mentioned reaction processes, other collisional reaction processes occurring in hydrogen plasmas and the interaction between the two chambers. Besides these rate equations, there are two constraints for each chamber: i.e., the charge neutrality and the particle number conservation. Thus, for the tandem two-chamber system, a set of 42 equations is solved numerically as a function of plasma parameters.

3. Numerical Results and Discussion

The procedure for numerical simulation is as follows: To determine the electron density dependence of H^- production, calculations are performed for various electron densities, $n_e(1)$, in the 1st chamber on the assumption that other plasma parameters are kept constant: i.e., for example, the electron density ratio between two chambers $n_e(2)/n_e(1) = 0.2$, density of e in the 1st chamber $n_{H^+}(1)/n_e(1) = 0.05$, $p = 0.67$ Pa (5 mTorr), T_e in the 1st chamber $T_e(1) = 5$ eV and T_e in the 2nd chamber $T_e(2) = 1$ eV, and the filter position $L_1:L_2 = 28:2$ cm. According to previously obtained results,[5,14] these plasma conditions were chosen to optimize H^- pure-volume production in the 2nd chamber. They are also used in the present study.

Fig. 3

Figure 3 shows the H^- densities, $H^-(2)$, in the 2nd chambers for various different values of P_{cs}. Wall conditions are as follows. For positive ions, $P_{cs1} = P_{cs2} = P_{cs3} = P_{cs}(+)$, and $P_{cs}(+) = 20 P_{csH} P_{eq} = P_1 = 0.01$, and $P_2 = P_3 = 0.3$. When $P_{csH} = 0$, i.e. curve (1), H^- ions are produced by the so-called two-step pure-volume process. With increasing P_{csH}, as was shown previously,[7,11]

$H^-(2)$ increases markedly. In a high density region, i.e. at $n_e(1) = 5\times10^{13}$ cm^{-3}, $H^-(2)$ is enhanced by a factor of four for curve (4) and by a factor of seven for curve (5). Since the same factor of enhancement was obtained when the effect of surface H^- production in only the 2nd chamber was taken into account, one can conclude that the 2nd chamber is the most effective area for surface enhancement of H^- production. In the present simulation, as the magnetic filter is set at L_1 = 28 cm, the total area of the wall surface in the 2nd chamber is nearly equal to the area of the end wall which corresponds to the plasma grid of the tandem volume sources.[3,4] Thus, the numerical results above mentioned agree well qualitatively with the experimental results.[3,4,9,10] As determined experimentally, the H^- yield rises with plasma grid temperature peaking at around 250 ℃[3] or 300 ℃.[4] This spatial or localized dependence of H^- production enhancement also supports the hypothesis that the H^- production enhancement is caused not by a volume process but by a surface process.

Theoretically, the probability, β^-, of incoming H atoms being converted to H^- ions on the wall is given as $\beta^- = (2/\pi)\exp[-\pi(\phi^- - A)/2av]$,[15] where ϕ^- is the work function, A is the electron affinity, a is the decay constant and v is the normal velocity of the incident particle. The effect of Cs is expressed through the value of ϕ^-. For example, ϕ^- is 1.45 eV for the surface covered with half of a monolayer of Cs and 2.1 eV for the surface covered with a monolayer of Cs. If we take the temperature of H atoms to be 0.5 eV, ϕ^- = 1.8 eV[9] and $a = 3.08\times10^{-5}$ eV · sec/m,[15,16] we can estimate $\beta^- = 4.87\times10^{-3}$ for H atoms. Impinging positive ions will be accelerated by sheath potential. Namely, positive ions have rather large v compared with H. For protons with energy of 1 eV, β^- is 2.05×10^{-2}. Therefore, the probability of incoming positive ions being converted to H^- ions on the wall could be much higher than that of thermal H atoms.[17] Then, in the present calculation, $P_{Cs}(+) = 2P_{CsH}$. Although P_{CsH} is treated as a numerical parameter, values of P_{CsH} are quite reasonable except that $P_{CsH} = 10^{-2}$. To

discuss Cs effects quantitatively, we must estimate precisely the relationship between P_{Cs} in our simulation and the theoretical value β^{-} for the corresponding experiment.

Figure 4 shows $H^{-}(2)$ as a function of p for various $n_e(1)$. In this calculation, the wall conditions are described by curve (4) in Fig. 3. In Fig. 4(a), i.e. in the absence of Cs, H^{-} ions are produced by a pure volume process. Apparently, there is an optimum pressure p_{opt} for each $n_e(1)$, and the value of p_{opt} increases with $n_e(1)$ (see the arrows in the figure). In experiment,[3,18] this is a typical tendency in a multicusp volume source where the parameter is not n_e but arc current I_A. On the other hand, in Fig. 4(b), i.e. in the presence of Cs, the pressure dependence of $H^{-}(2)$ for each $n_e(1)$ has almost the same pattern. As in the low-pressure region, enhancement of H^{-} production also appears clearly, the arrows which show the points where $H^{-}(2)$ corresponds to four times the value for $H^{-}(2)$ in the pure volume case shift to the low-pressure region. In this case, however, no optimum pressures are observed clearly. In experiment,[3,4] the H^{-} current is enhanced severalfold, and p_{opt} is reduced to 0.5-0.8 Pa and is almost constant irrespective of I_A or arc power P_{arc}. As described in ref.19, p_{opt} is reduced again to 0.3-0.4 Pa although p_{opt} increases gradually with P_{arc}. Figure 4 shows not the extracted H^{-} current but the H^{-} density in the 2nd chamber. On the other hand, experimental results, except those in ref.18, indicate the extracted H^{-} current as a function of p. Therefore, strictly speaking, we could not directly compare the numerical results with the experimental ones. Since the pressure dependence of H^{-} current depends strongly on stripping loss of H^{-} ions along the beam axis,[4,19] Nevertheless, as a whole, numerical results well reproduce the characteristic features of the experimental ones. Namely, the H^{-} current is enhanced by a large factor in a low-pressure region compared with the H^{-} current in the absence of Cs.

Figure 5 shows the production rate and destruction probability of $H^{-}(2)$

corresponding to the result in Fig. 4(b), where n_e = 5x10^{12} cm^{-3}. The predominant production process is surface production due to H. At p = 1 Pa, for example, both surface production due to H^+ and volume production VP have next dominant contribution, and the contribution of H_3^+ is the third. At p = 1 Pa, the density distribution of H^-:H_2^+:H_3^+ in the 2nd chamber is 49:24:27. According to Fig. 2, probability of H^- surface production from H_3^+ is effectively twofold larger than that from H_2^+. For destruction of H^- ions, electron detachments caused by H and H_2 are predominant for all regions. In the low-pressure region ($p \leq 1$ Pa), however, both electron detachment caused by H^+ and loss flux of negative ions $\Gamma_{2\rightarrow 1}$, i.e. flow of $H^-(2)$ across the filter to the 1st chamber, are predominant.

For discussion of the effect of electron cooling due to Cs injection, model calculation has been performed as a function of T_e of the 2nd chamber, $T_e(2)$. Here, wall condition is described by curve (4) in Fig. 3, and the parameter is $n_e(1)$. Numerical results are not shown here. For the pure volume case, $H^-(2)$ depends strongly on $T_e(2)$. With decreasing $T_e(2)$, $H^-(2)$ increases and then reaches the maximum value at about 1 eV.[14] On the other hand, in the presence of Cs, the enhancement of H^- production due to surface processes is so marked that the increase in H^- density due to a small reduction of T_e due to Cs injection could be masked. Therefore, electron cooling is not very effective for enhancing H^- yield, if plasma parameters including T_e are well optimized with the use of the magnetic filter. In experiment, however, electron cooling seems to be one of the reasons for the reduction in the electron-to-H^- ratio in the extracted beam.

4. Conclusions

We have theoretically studied cesium effects on enhancement of H^- yield and plasma parameter dependence of H^- density in negative-ion volume sources. The characteristic features of the experimental results obtained in the presence of cesium are well reproduced in the model. H^- surface production due to H and

positive ions (H^+ and H_3^+) contribute predominantly to H^- enhancement. For destruction of H^-, H and H_2 contribute predominantly. Detailed discussion including another wall effect of γ will be reported in a forthcoming paper.

This work was supported by a Grant-in-Aid for Scientific Research from the Ministry of Education, Science and Culture.

References

1) S.R.Walther, K.N.Leung and W.B.Kunkel: J.Appl.Phys. 64(1988)3424.

2) K.N.Leung, C.A.Hauck, W.B.Kunkel and S.R.Walther: Rev.Sci.Instrum. 60(1989)531.

3) Y.Okumura, M.Hanada, T.Inoue, H.Kojima, Y.Matsuda, Y.Ohara, M.Seki and K.Watanabe: *Proc. 5th Int. Symp. Production and Neutralization of Negative Ions and Beams*(AIP Press, NY, 1990) p.169.

4) A.Ando, T.Tsumori, Y.Oka, O.Kaneko, Y.Takeiri, E.Asano, T.Kawamoto, R.Akiyama and T.Kuroda: Phys. Plasmas 1(1994)2813.

5) O.Fukumasa and S.Ohashi: J.Phys.D 22(1989)1931.

6) O.Fukumasa: J.Appl.Phys. 71(1992)3193.

7) O.Fukumasa, T.Tanebe and H.Naitou: Rev.Sci.Instrum. 65(1994)1213.

8) J.R.Peterson: *Proc. 4th Int. Symp. Production and Neutralization of Negative Ions and Beams*(AIP Press, NY, 1989) p.113.

9) Y.Okumura, Y.Fujiwara, T.Inoue, K.Miyamoto, N.Miyamoto, A.Nagase, Y.Ohara and K.Watanabe: Rev.Sci.Instrum. 67(1996)1092.

10) K.N.Leung, C.F.A.van Os and W.B.Kunkel: Appl.Phys.Lett. 58(1991)1467.

11) O.Fukumasa and E.Niitani: *7th Int. Symp. Production and Neutralization of Negative Ions and Beams*(AIP Press, NY, 1995).

12) J.R.Hiskes and A.M.Karo: J.Appl.Phys. 67(1990)6621.

13) O.Fukumasa, K.Mutou and H.Naitou: Rev.Sci.Instrum. 63(1992)2693.

14) O.Fukumasa: J.Phys.D: Appl.Phys. 22(1989)1668.

15) B.Rasser, J.N.M.Van Wunnik and J.Los: Surf.Sci. 118(1982)697.

16) T.Okuyama: private communication(1992).

17) P.Berlemont, D.A.Skinner and M.Bacal: Chem.Phys.Lett. 183(1991)397.

18) C.Courteille, A.M.Bruneteau and M.Bacal: Rev.Sci.Instrum. 66(1995)2533.

19) Y.Takeiri, A.Ando, O.Kaneko, Y.Oka, K.Tsumori, R.Akiyama, E.Asano, T.Kawamoto, T.Kuroda, M.Tanaka and H.Kawakami: Rev.Sci.Instrum. 66(1995)2541.

Figure Captions

Fig. 1. Simulation model for the tandem two-chamber system.

Fig. 2. Reaction processes at the wall surface considered in modeling.

Fig. 3. Effects of the surface production due to both H atoms and positive ions on enhancement of H^- production: H^- density, $H^-(2)$, in the second chamber versus electron density in the first chamber $n_e(1)$. Parameter is the probability of H^- formation at the wall, P_{cs}.

Fig. 4. Effects of hydrogen gas pressure on H^- production: $H^-(2)$ versus gas pressure p, (a) without cesium, and (b) with cesium. In (a), the arrow shows the point where H^- density is maximum. In (b), the arrows show the points where H^- density corresponds to four times the H^- density in the absence of cesium.

Fig. 5. Production rates (a), and destruction probabilities (b) for $H^-(2)$ density versus p, corresponding to the results shown in Fig. 4(b), where $n_e = 5 \times 10^{12}$ cm^{-3}.

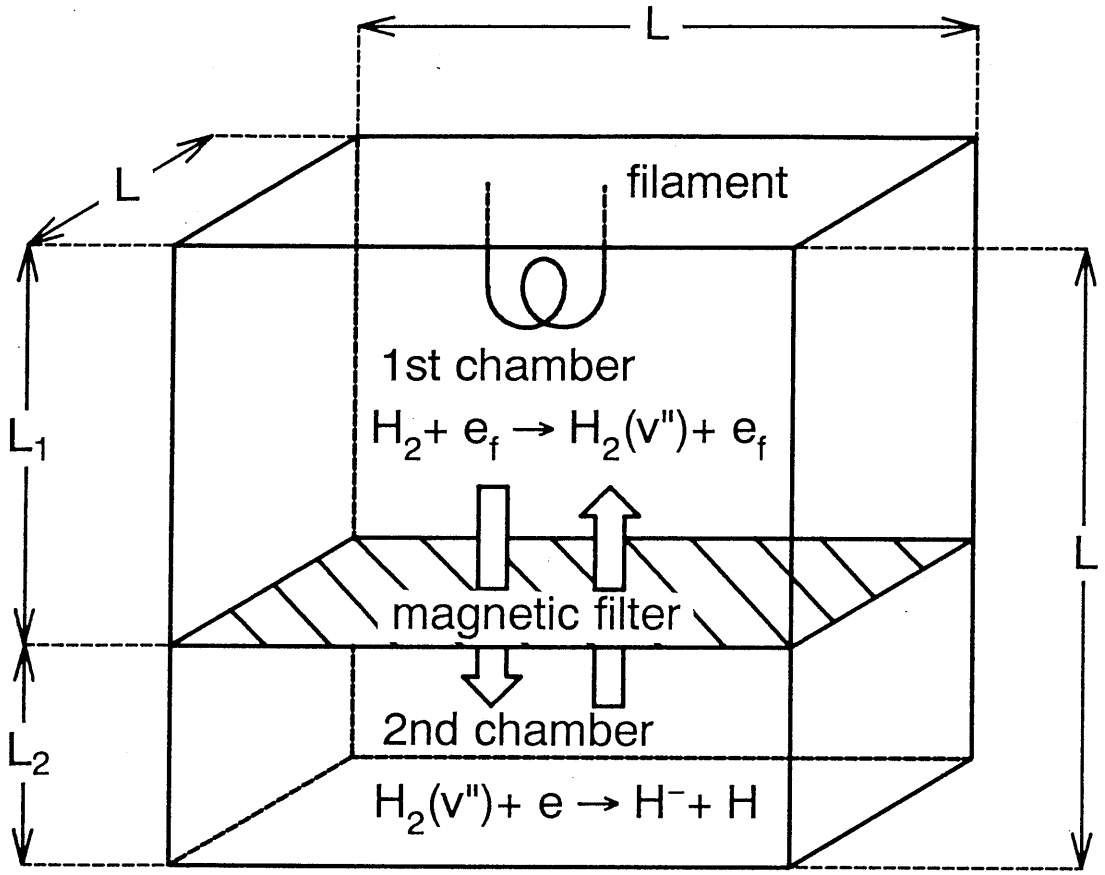

Fig.1 O. Fukumasa (5)

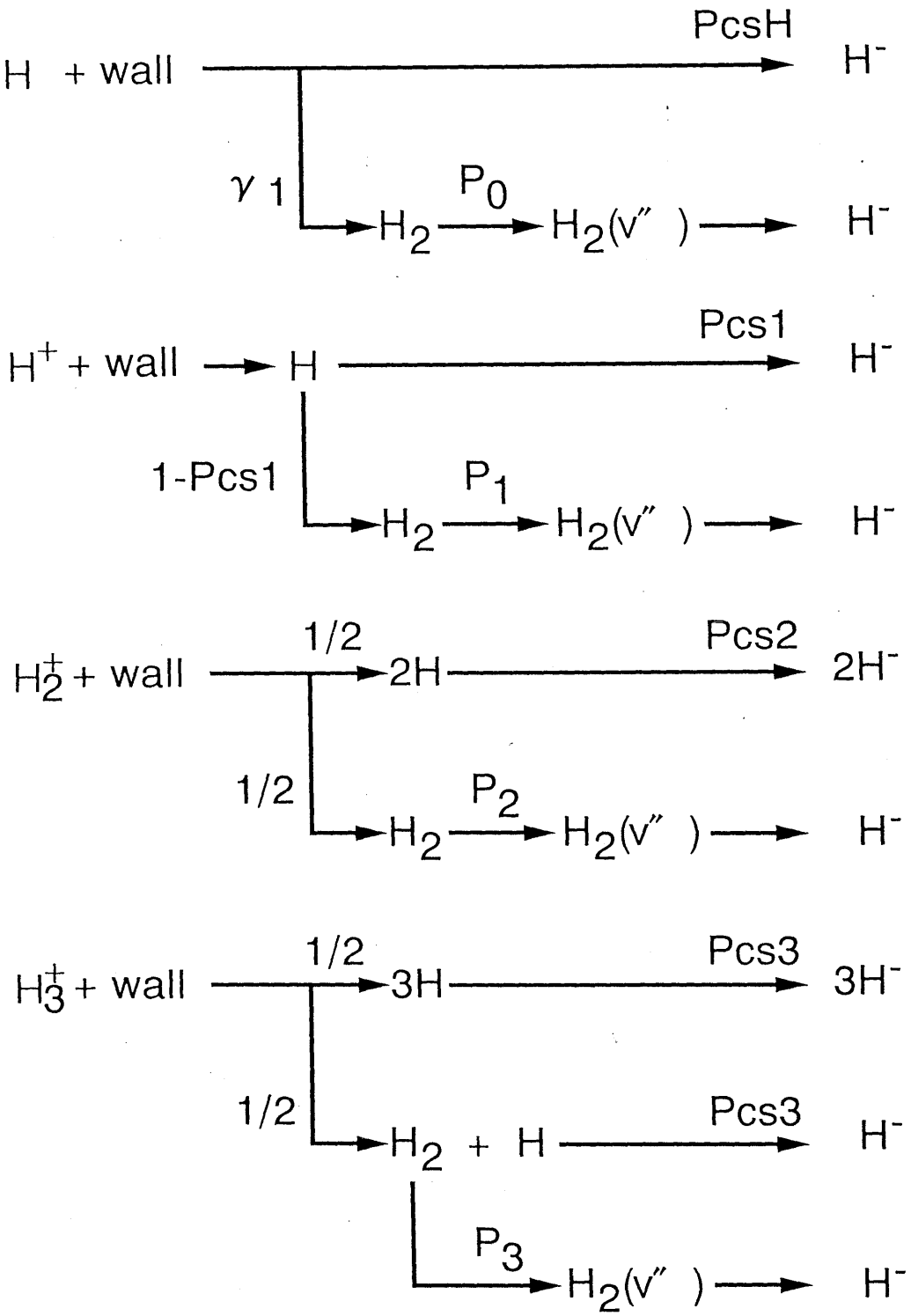

Fig. 2 O. Fukumasa (5)

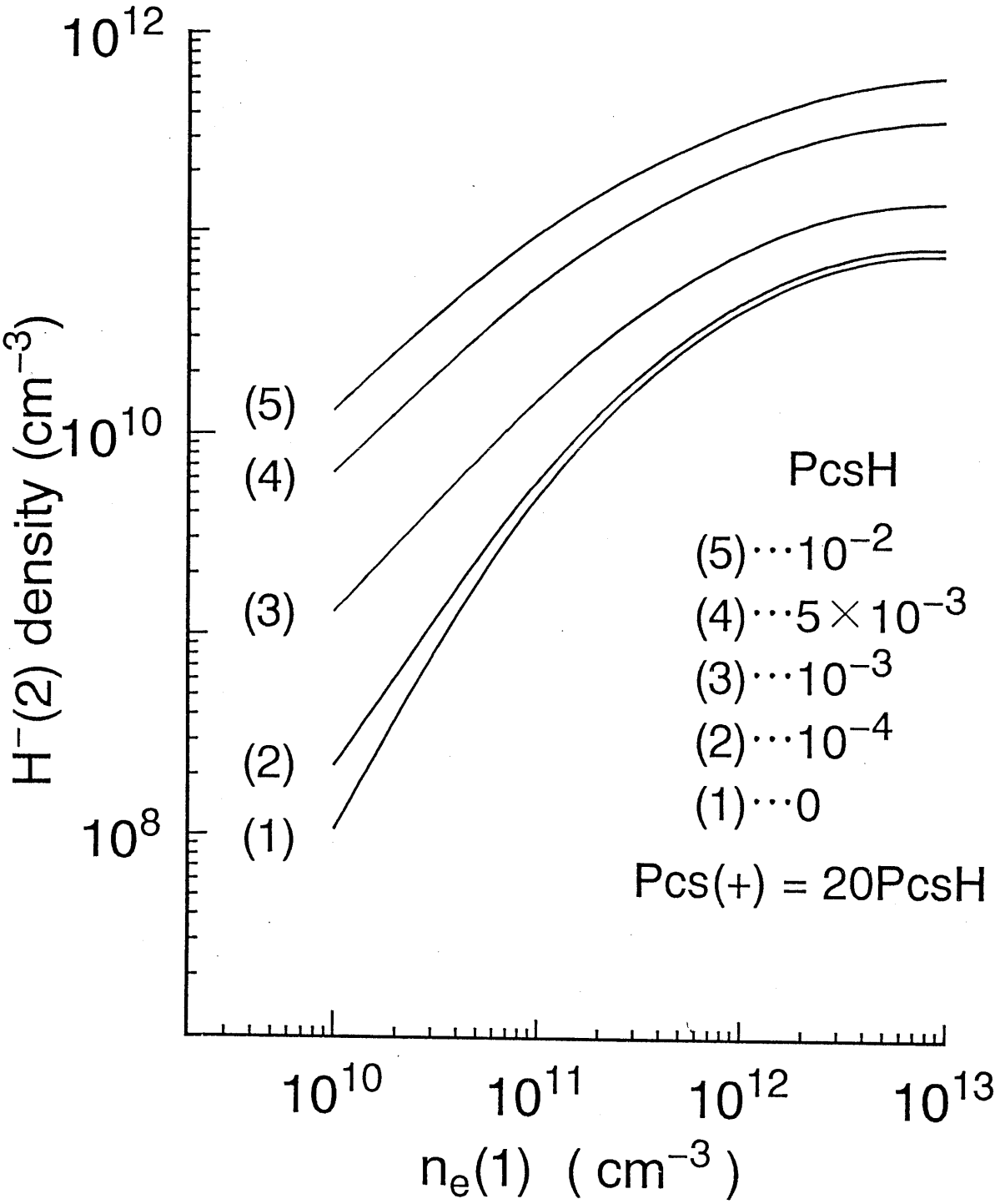

Fig.3 O. Fukumasa (5)

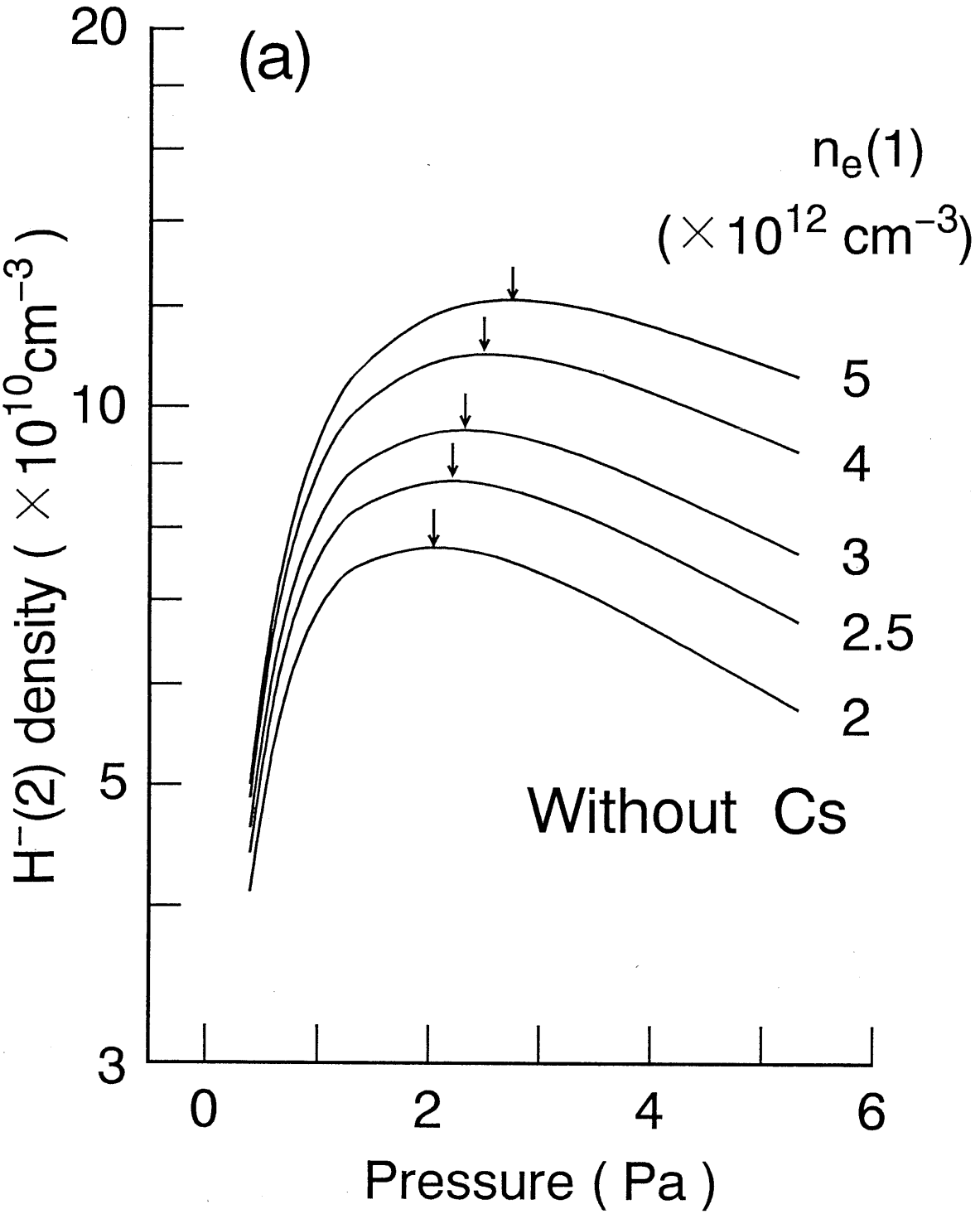

Fig. 4 O. Fukumasa (4)

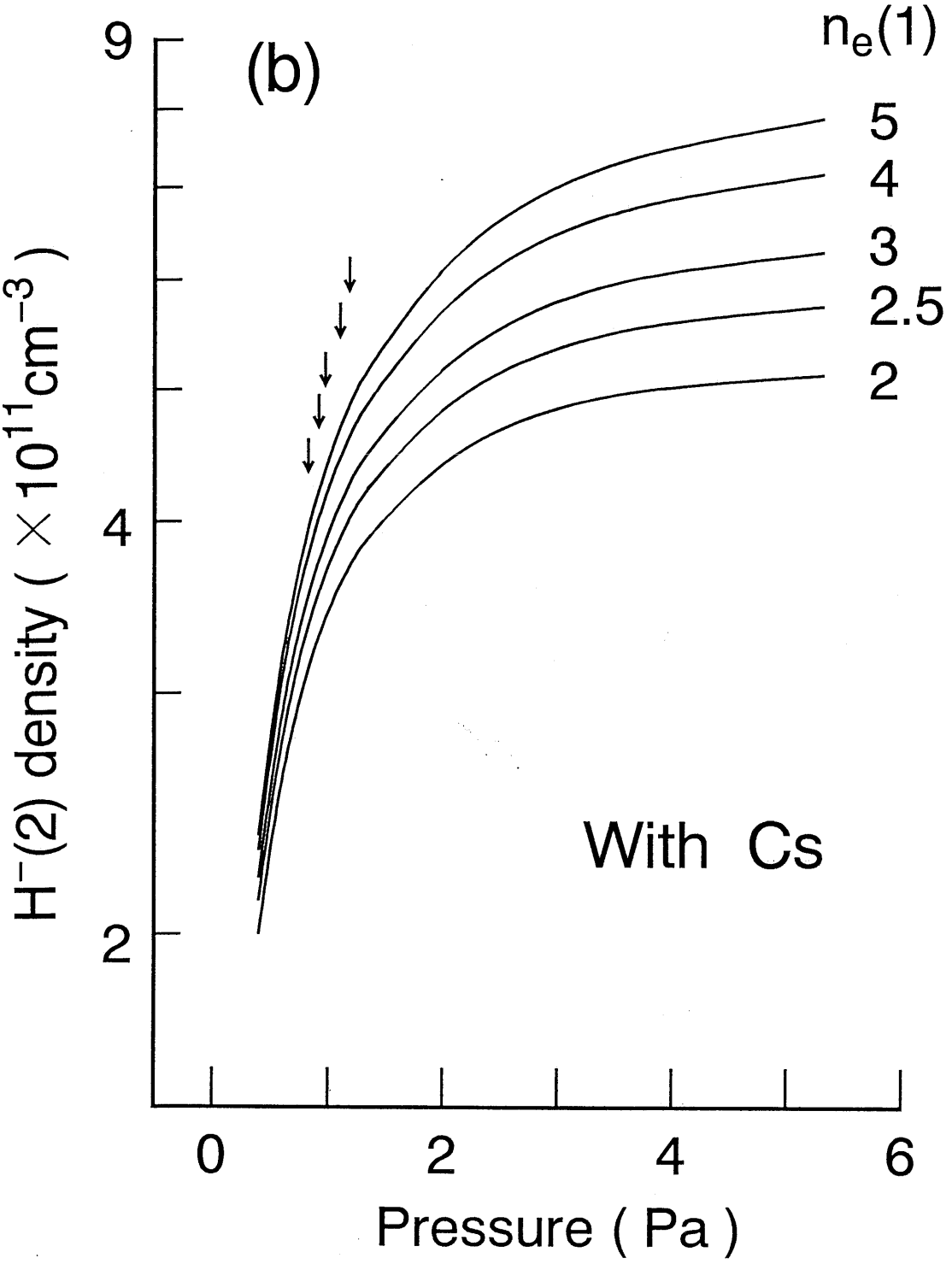

Fig. 4 O. Fukumasa (4)

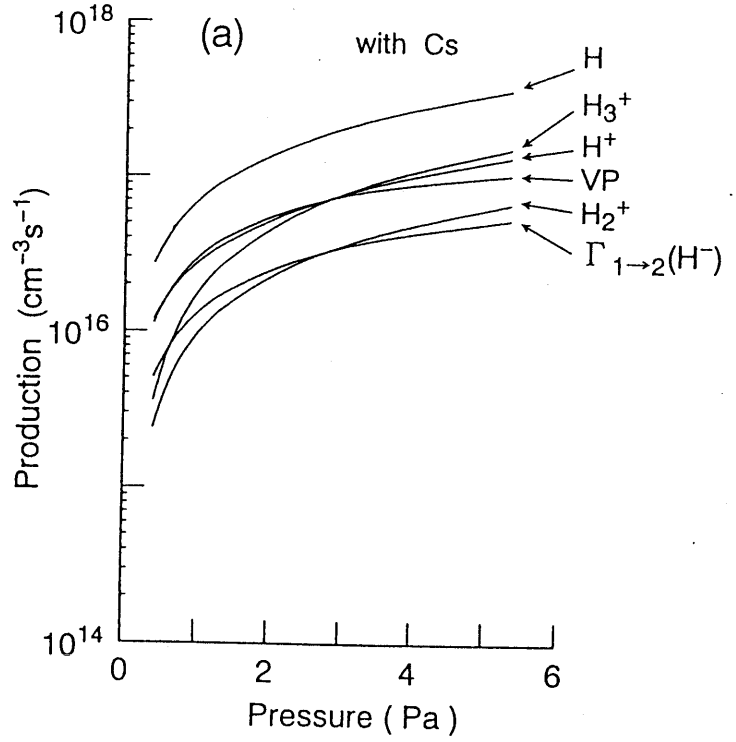

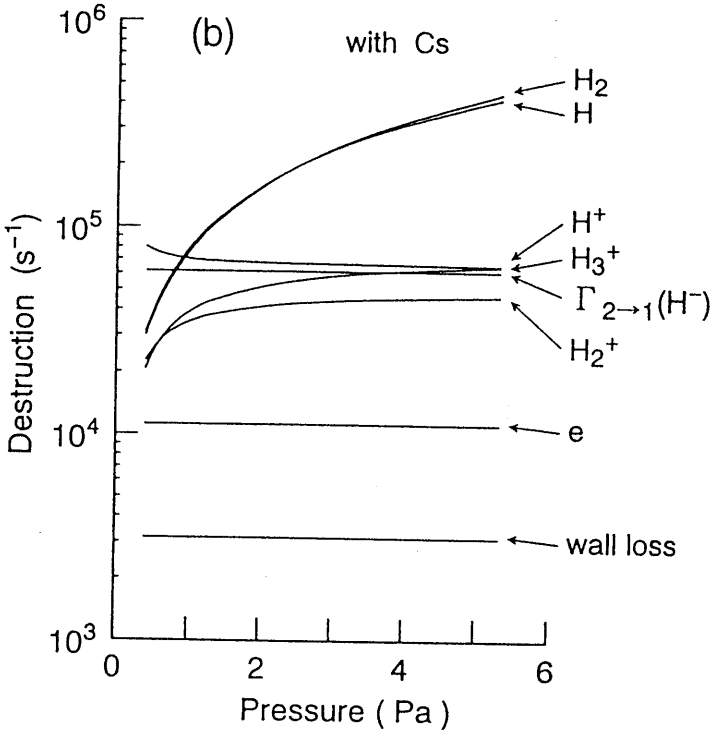

Fig.5 O. Fukumasa (5)